Thermodynamic Properties of $NiCr_2O_4$-$NiFe_2O_4$ Spinel Solid Solution

Bong-Hoon Park† and Dong-Su Kim*

†*Division of Metals Examination, Korea Industrial Property Office, Taejon 302-173, Korea*
Dept. of Environmental Sci. and Eng., Ewha Womans University, Seoul 120-750, Korea
Received April 4, 1999

The tie lines delineating ion-exchange equilibria between $NiFe_2O_4$-$NiCr_2O_4$ spinel solid solution and Fe_2O_3-Cr_2O_3 corundum solid solution were determined at 900, 1000, and 1200 °C by electron microprobe and energy dispersive X-ray analysis of oxide phases, using the flux growth technique. Activities of the spinel components were calculated from the tie lines, assuming Temkin's ideal mixing in the corundum solid solution. The spinel phase could be expressed by a regular solution with negative deviations from ideality. The Gibbs free energies of mixing for spinel solid solution were discussed in terms of the cation distribution model, based on site preference energies and assuming random mixing on both tetrahedral and octahedral sites.

Introduction

The spinel phases play an important role in the oxidation of alloy, formation of inclusions, and refining of metals. There have been extensive studies on thermodynamic properties of spinel solid solution and several attempts have been made to characterize the cation distribution in certain spinel systems and to relate thermodynamic properties to structure information.[1~4] One of the present authors[5] used a newly developed experimental technique for the determination of the tie lines delineating two phases, using the flux growth method based on Ostwald ripening mechanism. The aim of the present investigation is to provide an information on spinel-corundum phase relations in NiO-Fe_2O_3-Cr_2O_3 system and to obtain the activities for spinel phases whose data are not available in the literature. The Gibbs energies of mixing in spinel solid solution are calculated and compared with those obtained from a cation distribution model.[2]

Experimental Section

α-Fe_2O_3 (>99.99 wt.%) was purchased from Rare Metallic Co. and $Na_2B_4O_7$, Cr_2O_3, and NiO were all reagent grade (Aldrich Co.). An excess amount of these powders, about 1.5 times greater than the solubility predicted from the phase diagram, was mixed with the $Na_2O \cdot 2B_2O_3$ flux. The experiments were conducted in a vertical resistance furnace having SiC heating elements. The mixtures (15 g) in a Pt crucible were conditioned at the desired temperatures and stirred with a Pt stirrer (10 rad/sec) under dry air environment to make the homogeneous mixture. After standing for 2-8 hrs, the sample was quenched into water. No solid solution phases were precipitated on quenching. Contents of the spinel and corundum component in the crystal grains were determined using electron microprobe and energy dispersive X-rays (Hidachi, X650S) rather than wet chemical analysis, since it was difficult to separate the two phases. The strong point of this experimental method compared with conventional quenching method can be found in the fact that the elemental concentrations in the crystal grown in the solution are constant depending on time and they are in equilibrium resulting from homogeneous state. More detailed descriptions are given in the previous report.[5]

Results and Discussion

Tie line between corundum and spinel phases. The Fe_2O_3, NiO, and Cr_2O_3 crystals, with initial average sizes of 0.1-1.0 μm in saturated solution of $Na_2O \cdot 2B_2O_3$ flux, were found to grow to the size of 10-20 μm in a period of 2-8 hrs. The observed coarsening of crystals was considered to be due to the Ostwald ripening mechanism in which the driving force is the reduction of total interfacial energy of the larger crystals. More details of this mechnism are discussed elsewhere.[5] The corundum and spinel crystals were formed under equilibrium conditions during Ostwald ripening due to the low degree of supersaturation with respect to crystal growth. The experimental results for the equilibrium compositions are summarized in Table 1 and the tie lines delineating the spinel and corundum solid solution at 900, 1000, 1200 °C are shown in Figure 1.

As can be seen in Figure 1, the deviation from the stoichiometric spinel composition increases with an increase in temperature and tends to decrease with increasing nickel content. Tie lines in the region of Fe_2O_3-poor compositions could not be determined since the Na_2O-Fe_2O_3-Cr_2O_3 solid solution was observed to be formed. The contents of Na and B in both phases were analyzed to be less than 30 wt.ppm, respectively.

Stoichiometry of spinel solid solution. In the present experimental conditions, ferrous ions are produced as predicted from the previous works[6~9] concerning the phase equilibria in the ferrite region of Fe-Ni-O system as a function of temperature and oxygen partial pressure. Therefore, the experimental data should be plotted in the Fe_2O_3-FeO-Cr_2O_3-NiO quarternary system, not in the ternary system as shown in Figure 1. However, since the content of ferrous ion in the spinel solid solutions could not be determined by the present analytical method, the experimental data are plotted in the ternary system of Fe_2O_3-Cr_2O_3-NiO, assuming that the

Table 1. Tie-line compositions of $Ni_{0.5}CrO_2$-$Ni_{0.5}FeO_2$ and $FeO_{1.5}$-$CrO_{1.5}$ at 900, 1000, and 1200 °C (mol %)

Temp. (°C)	Corundum			Spinel		
	$x_{CrO1.5}$	$x_{FeO1.5}$	x_{NiO}	$x_{CrO1.5}$	$x_{FeO1.5}$	x_{NiO}
900	0.10	0.90	0	0.04	0.49	0.47
	0.22	0.78	0	0.08	0.44	0.48
	0.36	0.64	0	0.12	0.40	0.48
	0.68	0.32	0	0.21	0.32	0.47
	0.84	0.16	0	0.28	0.24	0.48
1000	0.08	0.92	0	0.03	0.50	0.47
	0.20	0.80	0	0.07	0.46	0.47
	0.31	0.69	0	0.10	0.41	0.49
	0.54	0.45	0.01	0.19	0.33	0.48
	0.68	0.31	0.01	0.22	0.28	0.50
	0.72	0.27	0.01	0.25	0.27	0.48
	0.76	0.23	0.01	0.27	0.25	0.48
1200	0.10	0.90	0	0.07	0.55	0.38
	0.23	0.77	0	0.14	0.47	0.39
	0.39	0.61	0	0.17	0.39	0.44
	0.56	0.41	0.03	0.24	0.33	0.43
	0.68	0.29	0.03	0.27	0.28	0.45

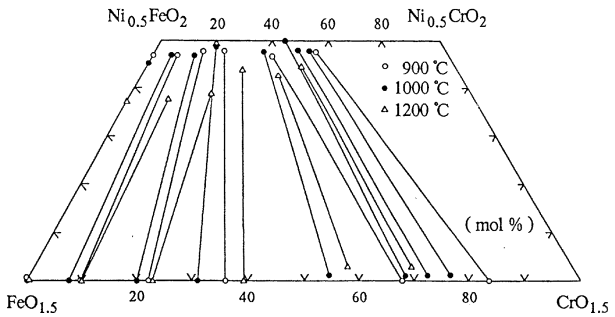

Figure 1. Phase diagram of the NiO-Fe_2O_3-Cr_2O_3 system, showing tie lines between spinel and corundum phases at 900, 1000, and 1200 °C.

analyzed Fe content is equal to that of ferric ion. It should be noted, therefore, that the standard state for $NiFe_2O_4$ is not the oxygen-saturated phase in equilibrium with Fe_2O_3. The data points at 900 and 1000 °C, having comparatively small deviation from stoichiometric spinel composition, were used for the calculation of activities in sipnel phase.

Activities of components in the spinel solid solution. When tie lines between two phases in equilibrium are known and activity data for one phase are available, the activities of the components in the second phase can be derived using the following modified Gibbs-Duhem integration method suggested by Wagner[10] and applied to oxide systems by Muan.[11] In the present calculation, $Ni_{0.5}FeO_2$, $Ni_{0.5}CrO_2$, $FeO_{1.5}$, and $CrO_{1.5}$ are used as the composition variables. Intracrystalline ion-exchange equilibrium is written as,

$$FeO_{1.5} \cdot Ni_{0.5}CrO_2 \rightleftharpoons Ni_{0.5}FeO_2\ CrO_{1.5} \quad (1)$$

and the modified Gibbs-Duhem integration is given by

$$\log\gamma_{Ni0.5FeO2} = \int_1^{x(Ni0.5FeO2)} x_{Ni0.5CrO2}\, d \log(a_{FeO1.5}x_{Ni0.5CrO2}/a_{CrO1.5}x_{Ni0.5FeO2}) \quad (2)$$

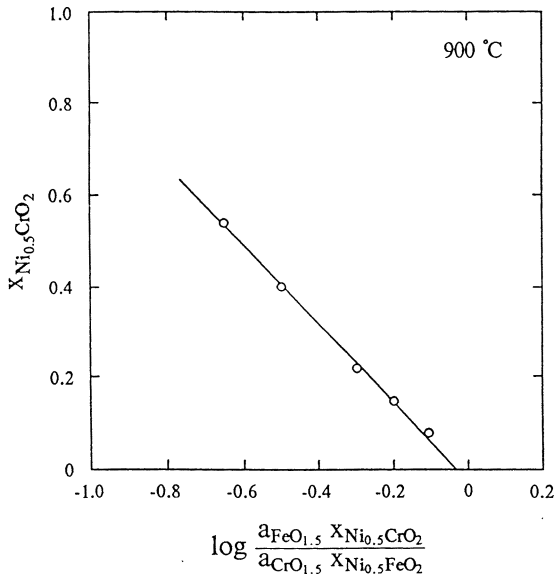

Figure 2. Modified Gibbs-Duhem integration plot at 900 °C.

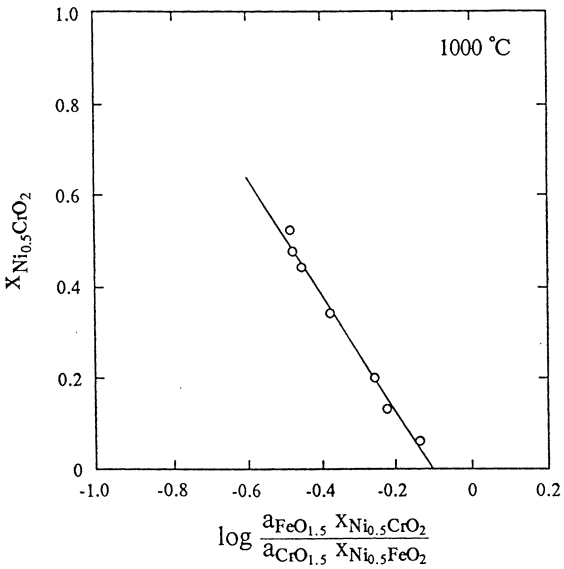

Figure 3. Modified Gibbs-Duhem integration plot at 1000 °C.

Mixing of the corundum solid solution is ideal according to the Temkin model; that is, activities of Cr_2O_3 and Fe_2O_3 will be equivalent to the square of their mole fractions.[11~17] This is further supported by the fact that Fe_2O_3 and Cr_2O_3 have the same crystal structure and the cations are nearly the same size - Cr^{3+} (0.615 Å) and Fe^{3+} (0.645 Å) - according to the Shannon and Prewitt scale[18] for six fold coordination.

The modified Gibbs-Duhem integration plot for $Ni_{0.5}CrO_2$ and $Ni_{0.5}FeO_2$ is shown in Figures 2 and 3. In these plots, mole fractions of $Ni_{0.5}CrO_2$ and $Ni_{0.5}FeO_2$ can be recalculated as $x_{Ni0.5CrO2} + x_{Ni0.5FeO2}$ 1. The value of $\log\gamma_{Ni0.5FeO2}$ is obtained by the area below integration in Figures 2 and 3, while $\log\gamma_{Ni0.5CrO2}$ can be evaluated from the area above the curve. However, there is a considerable uncertainty in extrapolating the logarithmic terms *vs.* $x_{Ni0.5CrO2}$ line to $x_{Ni0.5CrO2}$ 1 due to the lack of data at the Fe_2O_3-poor compositions. For this reason, the activities of $Ni_{0.5}CrO_2$ were deter-

mined by Gibbs-Duhem integration plot. The results are shown in Figure 4. It should be noted that the straight line indicated in Figures 2 and 3 suggests that the spinel solid solution is *regular*. The regular solution parameter, α, was determined either by the slope which is equal to $(RT/2\alpha)$ or the area which is equal to $\log\gamma_{Ni0.5FeO2} = \alpha x^2_{Ni0.5CrO2}/RT$. These values should be constant regardless of temperature, but those for obtained at 900 and 1000 °C are found to be –13.1 and –10.4 (kJ/mol), respectively.

Comparison with cation distribution model.[2] Distribution of cations between the tetrahedral and octahedral sites of pure spinels can be estimated from octahedral site preference energies, assuming ideal Temkin mixing of cations on each cation sublattice.[1~4] Jacob and Alcock[19] have shown that the cation distribution estimated from the site preference energies for a number of aluminate spinels is in good agreement with X-ray and neutron diffraction measurements. The approach used by Jacob and Alcock[2] is used to estimate the activity-composition relationship in the present intracrystalline ion-exchange equilibria between tetrahedral and octahedral sites. The values for the octahedral site preference energies for Ni^{2+} (–86.2 kJ/mol), Fe^{3+} (0 kJ/mol), and Cr^{3+} (–157.7 kJ/mol) obtained by Dunitz and Orgel[20] from crystal-field theory are used.

The intracrystalline ion-exchange equilibria can be written and the enthalpy change for the exchange equilibria, ΔH^{EX}, can be deduced from the site preference energies for $Ni_{0.5}CrO_2$.

$$(Ni^{2+}) + [Cr^{3+}] = (Cr^{3+}) + [Ni^{2+}] \; ; \; \Delta H^{EX} = 71.5 \text{ (kJ/mol)} \quad (3)$$

and for $Ni_{0.5}FeO_2$,

$$(Ni^{2+}) + [Fe^{3+}] = (Fe^{3+}) + [Ni^{2+}] \; ; \; \Delta H^{EX} -86.2 \text{ (kJ/mol)} \quad (4)$$

where ( ) and [ ] denote tetrahedral and octahedral sites, respectively. The cation distribution on octahedral sites is calculated from the solution to the following pair of equations:[2,21~23]

$$71.5 = -RT \ln (2[x_{Ni2+}] \{x_{NiCr2O4} - [x_{Cr3+}]\} / \{1-2[x_{Ni2+}]\}[x_{Cr3+}]) \quad (5)$$

$$86.2 = -RT \ln (2[x_{Ni2+}] \{x_{NiFe2O4} - [x_{Fe3+}]\} / \{1-2[x_{Ni2+}]\}[x_{Fe3+}]) \quad (6)$$

where $[x_i]$ and x_i represent the ion fraction on the octahedral site and mole fraction of each spinel component. The calculated results for the cation distributions are listed in Table 2.

The activities can be evaluated from the cation distribution values relative to a normal spinel for $Ni_{0.5}CrO_2$, and an inverse spinel for $Ni_{0.5}FeO_2$, as the standard state using the following equations:[12]

$$a_{Ni0.5CrO2} \{ [x_{Cr3+}](x_{Ni2+})^{1/2}\} / \{ [x_{Cr3+}]_o(x_{Ni2+})_o^{1/2}\} \quad (7)$$

$$a_{Ni0.5FeO2} \{ [x_{Fe3+}](x_{Fe3+})[x_{Ni2+}]^{1/2}\} / \{ [x_{Fe3+}]_o(x_{Fe3+})_o[x_{Ni2+}]_o \}^{1/2} \quad (8)$$

where $(\,)_o$ and $[\,]_o$ denote ion fractions in pure components.

The calculated results for activities of spinel components and Gibbs energy of mixing, ΔG^M, are given in Figures 4 and 5, indicating that the experimental values for ΔG^M are less negative than those of the model. The values for Gibbs energy of mixing in other spinel solid solutions with common cation, obtained by Jacob and co-workers,[13,21~23] are also included in Figure 5 for comparison along with those obtained at 1000 °C according to Temkin's law. It is of interest to note that the values for ΔG^M in the group of normal-normal spinel solid solution are approximately half the values in the group of normal-inverse spinel solid solution, except for the $Fe_{0.5}AlO_2$-$Fe_{1.5}O_2$ system.

Table 2. Calculated cation distributions based on cation distribution model

Composition	Tetrahedral site, Number of ions			Octahedral site, Number of ions		
$x_{Ni0.5FeO2}$	(Fe^{3+})	(Cr^{3+})	(Ni^{2+})	$[Fe^{3+}]$	$[Cr^{3+}]$	$[Ni^{2+}]$
0	0.000	4.655×10^{-2}	9.534×10^{-1}	0.000	1.953	0.046
0.1	0.200	7.943×10^{-3}	7.921×10^{-1}	1.526×10^{-5}	1.792	0.208
0.2	0.400	2.757×10^{-3}	5.973×10^{-1}	7.837×10^{-5}	1.597	0.403
0.3	0.600	1.081×10^{-3}	3.992×10^{-1}	2.624×10^{-4}	1.399	0.601
0.4	0.799	3.502×10^{-4}	2.006×10^{-1}	9.258×10^{-4}	1.200	0.799
0.5	0.983	1.979×10^{-5}	1.675×10^{-2}	1.677×10^{-2}	1.000	0.983
0.6	0.999	1.311×10^{-6}	1.439×10^{-3}	2.014×10^{-1}	0.800	0.999
0.7	0.999	4.172×10^{-7}	7.243×10^{-4}	4.007×10^{-1}	0.600	0.999
0.8	0.999	2.086×10^{-8}	4.836×10^{-4}	6.005×10^{-1}	0.400	1.000
0.9	1.000	8.941×10^{-9}	3.629×10^{-4}	8.004×10^{-1}	0.200	1.000
1.0	1.000	0.000	2.904×10^{-4}	1.000	0.000	1.000

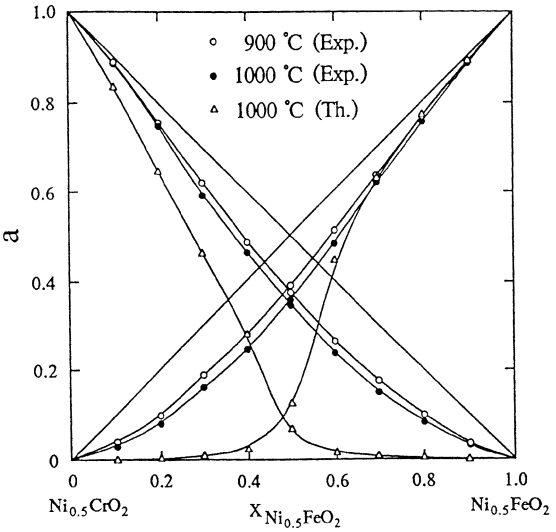

Figure 4. Activities for $Ni_{0.5}FeO_2$ and $Ni_{0.5}CrO_2$ in spinel solid solution at 900 and 1000 °C.

It has been shown that the correlation between experimentally derived and calculated Gibbs energy of mixing is very poor in most spinel solid solutions. Therefore, Jacob and co-workers[13,23] discussed the difference between theoretical and experimental values, $\Delta G^M_{th.} - \Delta G^M_{exp.}$, in terms of the lattice distortion effect due to cation size difference. The present results are shown in Figure 6, together with those obtained in other spinel solid solutions[13,21~23] with common cation. It can be seen that these values in the normal-inverse spinel solid solution increase in the order of $Ni_{0.5}CrO_2$-$Ni_{0.5}FeO_2$ > $Fe_{0.5}AlO_2$-$Fe_{1.5}O_2$ > $Fe_{0.5}CrO_2$-$Fe_{1.5}O_2$ which cannot be

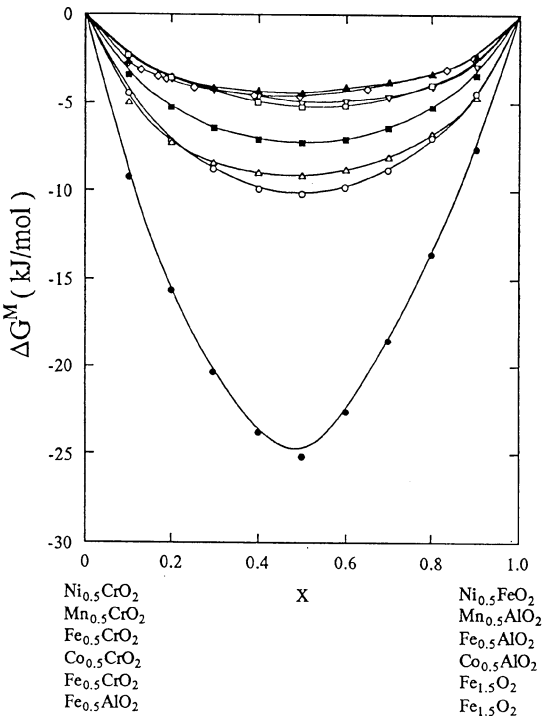

Figure 5. Gibbs energy of mixing $Ni_{0.5}FeO_2$-$Ni_{0.5}CrO_2$ at 1000 °C with the various spinel solution system: ● ; $Ni_{0.5}CrO_2$-$Ni_{0.5}FeO_2$ (Experimental), ○ ; $Ni_{0.5}CrO_2$-$Ni_{0.5}FeO_2$ (Theoretical), ◇ ; Temkin solution (1000°C), ▽ ; $Mn_{0.5}CrO_2$-$Mn_{0.5}AlO_2$, ■ ; $Fe_{0.5}CrO_2$-$Fe_{0.5}AlO_2$, ▲ ; $Co_{0.5}CrO_2$-$Co_{0.5}AlO_2$, □ ; $Fe_{0.5}AlO_2$-$Fe_{1.5}O_2$, △ ; $Fe_{0.5}CrO_2Fe_{1.5}O_2$.

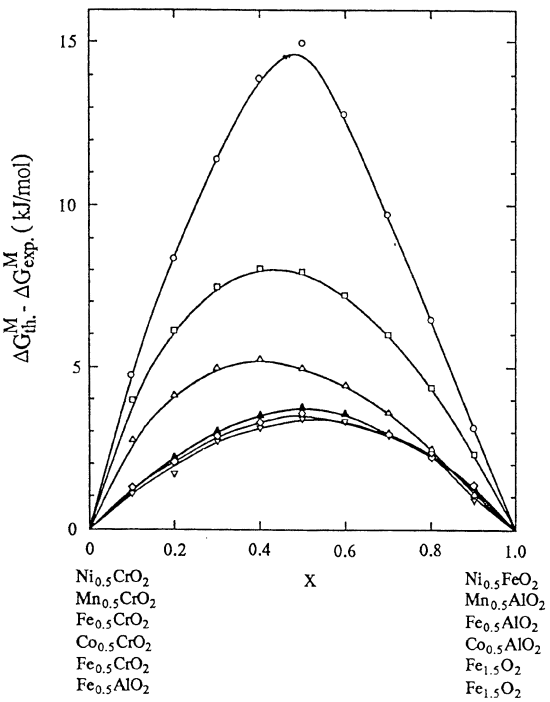

Figure 6. Difference in Gibbs energy of mixing between theoretical and experimental values. Symbols have same meaning as those in Figure 5.

explained by the cation size difference, whereas those in the normal-normal spinel solid solutions are approximately the same. It must be noted, however, that the cation distribution model proposed by O'Neill and Navrotsky,[4] in which the enthalpy of cation disordering, ΔH^{ex}, is not independent of the cation distribution in the spinel seems to be more reasonable for the explanation of thermodynamic propertis of spinel solid solutions. This model was not applied to the present results, because the present spinel solid solution has a significant width in the spinel field, and the parameters for this model were not accurately determined.

Conclusions

The activities for $Ni_{0.5}FeO_2$ and $Ni_{0.5}CrO_2$ spinel solid solution were determined from the experimental tie-line data at 900 and 1000 °C, thus, resulting in a regular solution with a negative deviation from ideality. The Gibbs energy of mixing in this system was found to be considerably less negative, compared with that derived from the cation distribution model based on site preference energies. The observed values for ΔG^M was found to be approximately twice as much as those observed in the normal-normal spinel solid solutions. The difference between experimental and theoretical Gibbs energy of mixing in the present system was greater than those observed in the previous spinel solid solutions.

References

1. Navrotsky, A.; Kleppa, O. J. *J. Inorg. Nucl. Chem.* **1967**, *29*, 2701.
2. Jacob, K. T.; Alcock, C. B. *J. Solid State Chem.* **1977**, *20*, 70.
3. O'Neill, H. S. C.; Navrotsky, A. *Am. Mineral.* **1983**, *68*, 181.
4. O'Neill, H. S. C.; Navrotsky, A. *Am. Mineral.* **1984**, *69*, 733.
5. Park, B.; Suito, H. *ISIJ Int.* **1990**, *30*, 426.
6. Shannon, R. D. *Acta Cryst.* **1976**, *A32*, 752.
7. Paladino, A. E. *J. Am. Ceram. Soc.* **1959**, *42*, 168.
8. Shafer, M. W. *J. Phys. Chem.* **1961**, *65*, 2055.
9. O'Bryan, H. M.; Monforte, F. R.; Blair, R. *J. Am. Ceram. Soc.* **1965**, *48*, 577.
10. Wagner, C. *Thermodynamics of Alloys*; Addison-Wesley: New York, 1955.
11. Muan, A. *Proc. Br. Ceram. Soc.* **1967**, *8*, 103.
12. Pelton, A. D.; Schmalzried, H.; Sticher, J. *J. Phys. Chm. Solids.* **1979**, *40*, 1103.
13. Petric, A.; Jacob, K. T. *J. Am. Ceram. Soc.* **1982**, *65*, 117.
14. Cremer, V. *N. Jb. Miner. Abh.* **1969**, *111*, 184.
15. Snethlage, R.; Klemm, D. *N. Jb. Miner. Abh.* **1975**, *125*, 227.
16. Schmahl, N. G.; Dillenburg, H. *Z. Phys. Chem. N. F.* **1969**, *65*, 119.
17. Katsura, T.; Nakihara, M.; Hara, S.; Sugihara, T. *J. Solid State Chem.* **1975**, *13*, 107.
18. Shannon, R. D.; Prewitt, C. T. *Acta Crystallogr. Sect. B.* **1969**, *25*, 925.
19. Jacob, K. T.; Alcock, C. B. *Met. Trans.* **1975**, *6B*, 215.
20. Dunitz, J. D.; Orgel, L. E. *J. Phys. Chem. Solids.* **1957**, *3*, 318.
21. Petric, A.; Jacob, K. T.; Alcock, C. B. *J. Am. Ceram. Soc.* **1981**, *64*, 632.
22. Petric, A.; Jacob, K. T. *Solid State Ionics* **1982**, *6*, 47.
23. Jacob, K. T.; Iyengar, G. N. K. *J. Am. Ceram. Soc.* **1986**, *69*, 487.